

Foatic actions of the symmetric group and fixed-point homomesy

Michael La Croix

Tom Roby

12 March 2024

Abstract

We study maps on the set of permutations of n generated by the Rényi-Foata map intertwined with other dihedral symmetries (of a permutation considered as a 0-1 matrix). Iterating these maps leads to dynamical systems that in some cases exhibit interesting orbit structures, e.g., every orbit size being a power of two, and homomesic statistics (ones which have the same average over each orbit). In particular, the number of fixed points (aka 1-cycles) of a permutation appears to be homomesic with respect to three of these maps, even in one case where the orbit structures are far from nice. For the most interesting such “Foatic” action, we give a heap analysis and recursive structure that allows us to prove the fixed-point homomesy and orbit properties, but two other cases remain conjectural.

1 Introduction

1.1 The Rényi-Foata Map on permutations

A well-known bijection \mathcal{F} from the symmetric group \mathfrak{S}_n to itself, due to Rényi [15, §4] and Foata-Schützenberger [6, pp. 13–15], simply takes a permutation given in a canonical disjoint cycle decomposition, drops the parentheses, and reinterprets the result as a permutation in one-line notation. (See (1) for an example.) Although not respecting the algebraic structure of \mathfrak{S}_n , it provides insight into combinatorial properties of permutations. For example it shows that among permutations in \mathfrak{S}_n , the number with exactly k *cycles* (counted by signless Stirling numbers of the first kind) is the same as the number with exactly k *left-to-right maxima*, which we call here **records** for short, and that the number with k *ascents* (counted by Eulerian numbers) is the same as the number with $k + 1$ *weak excedances*.

Definition 1. Let $w \in \mathfrak{S}_n$. The **canonical (disjoint) cycle decomposition (CCD)** of w is the decomposition of the bijection w into disjoint cycles, where (a) each cycle is written with its largest element first and (b) the cycles are written in increasing order of first (largest) elements. The **Rényi–Foata map** $\mathcal{F} : \mathfrak{S}_n \rightarrow \mathfrak{S}_n$ simply removes the parentheses from the CCD of w and regards the resulting word as a permutation in one-line notation.

For example:

$$w = 847296513 = (42)(6)(81)(9375) \xrightarrow{\mathcal{F}} 426819375 = (2)(95148736), \quad (1)$$

where the input and output to \mathcal{F} are each written both in one-line notation and CCD. Note that here w has 4 cycles, and $\mathcal{F}(w)$ has 4 records (viz., 4, 6, 8, and 9).

It is easy to see that \mathcal{F} is a bijection, whose inverse is given as follows. Take a permutation w given in one-line notation, place a left parenthesis before each record, then place corresponding right parentheses (one before each internal left parenthesis and after the last element).

Every permutation w has multiple representations, and we use whichever one is convenient at the moment. Ironically, from a computer science (or even just hand computational) standpoint, the conversion between different representations of the same w requires more effort than the map \mathcal{F} itself.

For a broader overview of this corner of permutation enumeration and its history, we direct the reader to the text of Stanley [19, §1.3] and the discussion of references in that chapter. Therein our map $w \mapsto \mathcal{F}(w)$ is called the *fundamental bijection* (translating the term “transformation fondamentale” of [6]) and denoted $w \mapsto \hat{w}$. Bona’s text [3, §3.3.1] is another useful reference.

1.2 Dynamics of permutation bijections

We consider certain cyclic actions on the symmetric group that are generated as an intertwining of the Rényi-Foata map \mathcal{F} with other involutive dihedral symmetries on \mathfrak{S}_n (via permutation matrices). In particular, we consider actions generated by maps of the following form:

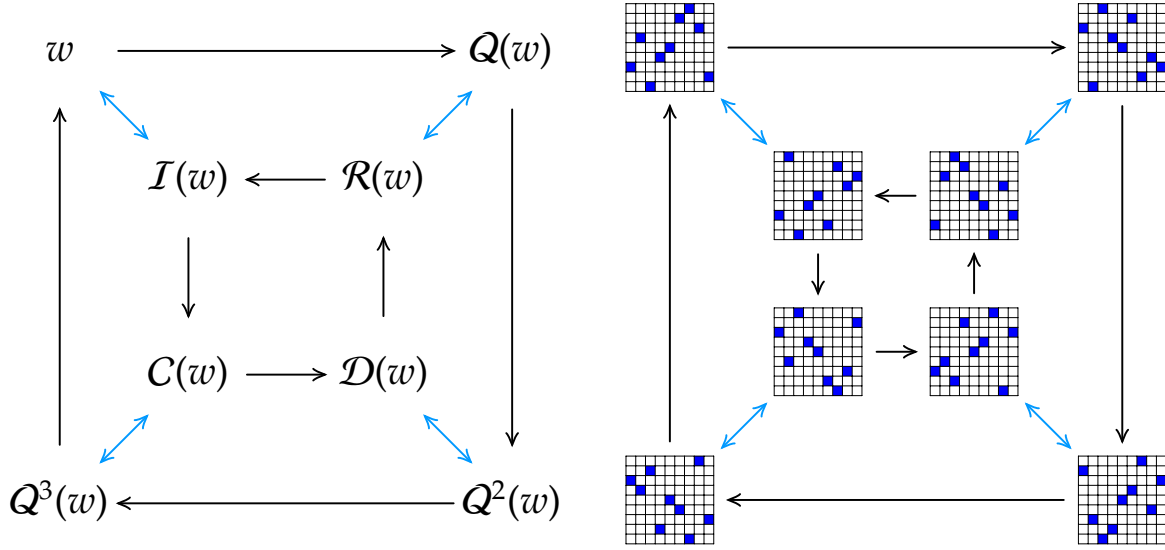
$$\mathfrak{S}_n \xrightarrow{\mathcal{F}} \mathfrak{S}_n \xrightarrow{\mathcal{A}} \mathfrak{S}_n \xrightarrow{\mathcal{F}^{-1}} \mathfrak{S}_n \xrightarrow{\mathcal{B}} \mathfrak{S}_n \quad (2)$$

where \mathcal{A} and \mathcal{B} are dihedral involutions, defined below.

Definition 2. For completeness, we name the five **dihedral involutions** of \mathfrak{S}_n as follows:

- (a) $\mathcal{C} : \mathfrak{S}_n \rightarrow \mathfrak{S}_n$, which takes a permutation $w = w_1 \dots w_n$ to its **complement** whose value in position i is $n + 1 - w_i$;
- (b) $\mathcal{R} : \mathfrak{S}_n \rightarrow \mathfrak{S}_n$, which takes a permutation $w = w_1 \dots w_n$ to its **reversal** whose value in position i is w_{n+1-i} ;
- (c) $\mathcal{Q}^2 : \mathfrak{S}_n \rightarrow \mathfrak{S}_n$, which takes a permutation $w = w_1 \dots w_n$ to its **rotation by 180-degrees**, whose value in position i is $n + 1 - w_{n+1-i}$. (We reserve \mathcal{Q} to denote the dihedral symmetry **rotation of (the permutation matrix of) w by 90-degrees counterclockwise**.)
- (d) $\mathcal{I} : \mathfrak{S}_n \rightarrow \mathfrak{S}_n$, which takes a permutation w to its **inverse** w^{-1} ;
- (e) $\mathcal{D} : \mathfrak{S}_n \rightarrow \mathfrak{S}_n$, which takes a permutation w to its **rotatedInverse** $\mathcal{Q}^2(\mathcal{I}(w))$.

Figure 1: The dihedral symmetries on \mathfrak{S}_n



The left image shows the dihedral group presented in terms of generators Q (black) and I (blue). Its actions the permutation graph of $w = 361458972$ are shown on the right. Note that Q corresponds to a counter-clockwise rotation of permutation matrices, but this induces a clockwise rotation of the corresponding graphs.

Of course, some of these maps can be obtained as compositions of others, e.g., $Q^2 = C \circ R = R \circ C$. Figure 1 summarizes the relationships between the dihedral involutions by presenting each in terms of the generators Q (black) and I (blue).

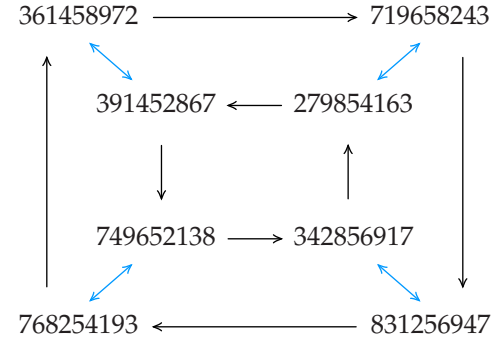
For humans, the first two operations (C and R) are easy to compute on permutations in one-line notation, but not in CCD. Taking the inverse of w in CCD is easy, since one just reverses the order of non-maximal elements in each cycle, but harder in one-line notation. $Q^2(w)$ is easy to compute in CCD: one simply complements each element of each cycle. The result will be a cycle-decomposition that is not CCD in general, but is easy to convert to CCD. In one-line notation $Q^2(w)$ also easy: one reads off the complement of each element of w from right-to-left. The operators R , C , and Q^2 act naturally on one-line presentation of permutations, while I , D , and Q^2 act naturally on the CCD.

Definition 3. We call the invertible maps defined as the fourfold composition in (2), where \mathcal{A} and \mathcal{B} are from the above list, **Foatic**. This gives a total of 25 different Foatic maps to study.

As part of our investigation we occasionally permitted \mathcal{A} and \mathcal{B} to act as Q , Q^3 , or the identity, but these additional actions did not produce any interesting results from the perspective of our investigation into homomesy. By excluding Q and Q^3 from our definition, we preserve the potentially useful fact that every Foatic action factors as a product of two involutions. In fact, the most tractable actions seemed to occur only when \mathcal{A} acted naturally on one-line presentations and \mathcal{B} acted naturally on CCD, although Sheridan Rossi later identified statistics of interest for all five possibilities of \mathcal{A} and \mathcal{B} summarized in Appendix A of [18].

Example 4. Let $w = 361458972$ (in one-line notation) $= (31)(4)(5)(92687)$ in CCD. Then

- (a) $\mathcal{C}(w) = 749652138 = (5)(624)(71)(983)$,
- (b) $\mathcal{R}(w) = 279854163 = (5)(648)(712)(93)$,
- (c) $\mathcal{Q}^2(w) = 831256947 = (5)(6)(84231)(97)$,
- (d) $\mathcal{I}(w) = 391452867 = (31)(4)(5)(97862)$, and
- (e) $\mathcal{D}(w) = 342856917 = (5)(6)(81324)(97)$.



It is worth noting that any Foatic map can be thought of as a product of two involutions $\mathcal{B} \circ \mathcal{F}^{-1} \circ \mathcal{A} \circ \mathcal{F} = \mathcal{B}(\mathcal{F}^{-1} \mathcal{A} \mathcal{F})$, where one of our dihedral involutions has been conjugated by \mathcal{F} . It will also be convenient in some cases to consider these actions to be starting partway through the composition, e.g., as $\mathcal{F}^{-1} \mathcal{A} \mathcal{F} \mathcal{B}$, considering such a conjugate action will produce the same orbit structure, but with potentially different homomesic statistics.

Example 5. If $\mathcal{A} = \mathcal{C}$ and $\mathcal{B} = \mathcal{I}$, then we get the Foatic map $\gamma := \mathcal{I} \circ \mathcal{F}^{-1} \circ \mathcal{C} \circ \mathcal{F}$. If $n = 5$, then $\gamma[(4213)(5)] = (2)(4)(513)$ as follows

$$w = (4213)(5) \xrightarrow{\mathcal{F}} 42135 \xrightarrow{\mathcal{C}} 24531 \xrightarrow{\mathcal{F}^{-1}} (2)(4)(531) \xrightarrow{\mathcal{I}} (2)(4)(513) = \gamma(w).$$

The orbit (of size six) generated by the above w is

$$w = (4213)(5) \xrightarrow{\gamma} (2)(4)(513) \xrightarrow{\gamma} (412)(53) \xrightarrow{\gamma} (2)(5314) \xrightarrow{\gamma} (431)(52) \xrightarrow{\gamma} (2)(3)(541) \xrightarrow{\gamma} w$$

1.3 The homomesy phenomenon

The homomesy phenomenon was first isolated by Propp and the second author [12] around 2011. Given a group action on a set of combinatorial objects, a statistic on these objects is called **homomesic** if its average value is the same over all orbits. More precisely:

Definition 6. Given a set S , an invertible map τ from S to itself such that each τ -orbit is finite, and a function (or “statistic”) $f : S \rightarrow \mathbb{K}$ taking values in some field \mathbb{K} of characteristic zero, we say the triple (S, τ, f) exhibits **homomesy** iff there exists a constant $c \in \mathbb{K}$ such that for every τ -orbit $\mathcal{O} \subset S$

$$\frac{1}{\#\mathcal{O}} \sum_{x \in \mathcal{O}} f(x) = c. \quad (3)$$

In this situation we say that the function $f : S \rightarrow \mathbb{K}$ is **homomesic** under the (cyclic) action of τ on S , or more specifically **c-mesic**.

When S is a finite set, homomesy can be restated equivalently as all orbit-averages being equal to the global average:

There are many examples of this phenomenon, of varying degrees of difficulty, in both older and more recent combinatorially work; see [16] for a survey. In particular, in many cases it has been fruitful to investigate actions that can be viewed as the composition of involutions on the set of objects. These include *promotion* of semi-standard Young tableaux [2] and *rowmotion* on the set of antichains or order ideals of certain posets [1, 20, 22], (particularly *minuscule*) posets [17]. Extensions include looking at certain more general products of *toggling* involutions (see [21]) in a variety of contexts, including non-crossing partitions [5], independent sets of a path graph [9], antichains [11]. Liftings of these combinatorial maps to the piecewise-linear setting of polytopes and further (via detropicalization) to the birational (and even noncommutative) realms are also of interest [4, 8, 7, 10].

While homomesic statistics can often be found in situations which give interesting examples of the *cyclic sieving phenomenon* of Reiner, Stanton, and White [13, 14], they also turn up for actions whose orbit structure is not well behaved. In particular, data strongly suggests that the Foatic complement-rotation map ρ of Section 4 has homomesic fixed-point statistic despite its orbit structure. The “Coxeter-toggling” of independent sets of a path graph [9] is another example with proven homomesy but where the orbit structures are too messy to find nice cyclic sieving.

1.4 Summary of the paper

This paper had its origin in James Propp’s vision to look for natural homomesies among basic combinatorial objects, particularly those counted by Rota’s Twelvelfold Way [19, §1.9]. In this first section we give background and define the basic setup. In Section 2, we give a careful study of reversal-inclusion, the most interesting Foatic map. In this situation, we use *heaps*, a kind of decreasing binary tree, to understand the recursive nature of the map. This allows us to prove some properties of the orbit structure, and find several homomesic statistics, including the natural statistic Fix on \mathfrak{S}_n which counts the number of fixed points (1-cycles) of a permutation.

In Sections 3, 4, and 5 we consider three other Foatic maps, complement-inversion, complement-rotation, and reversal-rotation, which appear conjecturally to have Fix as a homomesic statistic. The former also seems to have nice orbits. We give data to support the conjectures which remain open. Finally, in Section 6, we note that computer-generated data shows that none of the other 21 possible Foatic maps exhibits homomesy for Fix .

In her doctoral dissertation (supervised at UConn by the second author), Elizabeth Sheridan Rossi searched for homomesy for (linear combinations of) a wider range of permutation statistics under Foatic actions. For example, let $\text{Fix}_i(w)$ be the indicator function that takes the value 1 if $w_i = i$ and 0 otherwise. Then $\text{Fix}_1 - \text{Fix}_n$ is homomesic for 13 of the 25 Foatic maps. Call $i \in [n]$ an **excedance** if $w_i > i$ and a **weak excedance** if $w_i \geq i$; set $\text{exc } w = \text{number of excedances}$ and $\text{wexc} = \text{number of weak excedances}$ of $w \in \mathfrak{S}_n$. Sheridan Rossi proves that $\text{wexc} + \text{exc}$ is homomesic for inversion-inversion, rotation-inversion and rotation-rotation. She conjectures that wexc is homomesic for complement-rotatedInverse and reversal-rotatedInverse. See Appendix A for a summary and Chapter 2 of [18] for more information.

In the same dissertation, Sheridan Rossi considered a variant on the above setup, replacing the Rényi–Foata map \mathcal{F} with the Foata–Schützenberger map \mathcal{S} . The latter map is a (somewhat complicated) bijection on \mathfrak{S}_n with the property that $\text{maj}(w) = \mathcal{I}\mathcal{S}(w)$. It gave the first bijective proof that the statistics maj and \mathcal{I} are equidistributed on \mathfrak{S}_n (a result first obtained by MacMahon). See [19, §1.4] for further background. Let $D_i(w)$ be the indicator function of whether $i \in [n]$ is a descent of $w \in \mathfrak{S}_n$. Among other homomesies, Sheridan Rossi proved that $D_1 + D_{n-1}$ is homomesic for five such intertwining, and conjectured that this extends to $D_i + D_{n-i}$ for $1 < i < n$. See Appendix B for a summary and Chapter 3 of [18] for more information.

1.5 Acknowledgments

The authors are particularly grateful to James Propp, who first suggested this line of inquiry and noticed that the number of fixed points is a homomesic statistic for a few of the Foatic maps we consider here. We also greatly appreciate conversations we’ve had with Ira Gessel, and Darij Grinberg. David Einstein, Michael Joseph, and Elizabeth Sheridan Rossi all read early drafts of this paper, finding errors and contributing insightful comments. Exploratory computations were carried out in the PostScript programming language, and later confirmed by Sage code written by David Einstein. This collaboration began when the first author was a postdoc and the second a research affiliate in the mathematics department at MIT, whose hospitality we gratefully acknowledge.

2 Reversal-inversion

The Foatic action with the nicest orbit structures and properties is the one given by:

$$\overline{\varphi} : \mathfrak{S}_n \xrightarrow{\mathcal{F}} \mathfrak{S}_n \xrightarrow{\mathcal{R}} \mathfrak{S}_n \xrightarrow{\mathcal{F}^{-1}} \mathfrak{S}_n \xrightarrow{\mathcal{I}} \mathfrak{S}_n. \quad (4)$$

It turns out to be easier to study its conjugate map:

$$\varphi : \mathfrak{S}_n \xrightarrow{\mathcal{R}} \mathfrak{S}_n \xrightarrow{\mathcal{F}^{-1}} \mathfrak{S}_n \xrightarrow{\mathcal{I}} \mathfrak{S}_n \xrightarrow{\mathcal{F}} \mathfrak{S}_n \quad (5)$$

and to use the representation of permutations as *heaps*, aka *decreasing binary trees* [19, §1.5]. The action of φ (equivalently $\overline{\varphi}$) transforms the heap in an easily described way that preserves the isomorphism class of the underlying unlabeled tree. As a result we get a simple recursive structure of how φ acts on permutations of n in one-line notation, i.e., $\varphi(AnB) = Bn\varphi(A)$, where A and B are partial permutations (also in one-line notation). This allows us to prove that the statistic Fix on \mathfrak{S}_n that counts the number of fixed points is 1-mesic, and also show that all the orbit sizes are powers of 2 (Theorem 14).

Example 7. Let $w = (2)(43)(51) \in \mathfrak{S}_5$ in CCD. Then the successive action of $\overline{\varphi}$ on w is

detailed below:

$$\begin{aligned}
w = (2)(43)(51) &\mapsto 24351 \mapsto 15342 \mapsto (1)(5342) \mapsto (1)(5243) = \overline{\varphi}(w) \\
(1)(5243) &\mapsto 15243 \mapsto 34251 \mapsto (3)(42)(51) \mapsto (3)(42)(51) = \overline{\varphi}^2(w) \\
(3)(42)(51) &\mapsto 34251 \mapsto 15243 \mapsto (1)(5243) \mapsto (1)(5342) = \overline{\varphi}^3(w) \\
(1)(5342) &\mapsto 15342 \mapsto 24351 \mapsto (2)(43)(51) \mapsto (2)(43)(51) = \overline{\varphi}^4(w)
\end{aligned}$$

This example also displays (down the second column) the conjugate orbit of φ , also of size 4.

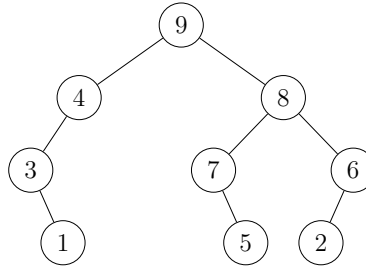
$$24351 \xrightarrow{\varphi} 15243 \xrightarrow{\varphi} 34251 \xrightarrow{\varphi} 15342 \mapsto$$

Larger examples with two orbits from the $\overline{\varphi}$ -actions on \mathfrak{S}_7 and \mathfrak{S}_9 are given in Figure 3.

Definition 8. Let S be a finite totally ordered set, and $w \in \mathfrak{S}_S$ a permutation of S written in one-line notation. If $S \subseteq [n] := \{1, 2, \dots, n\}$, we call w a **partial permutation of n** . We recursively define the **heap** of w , $H(w)$ as follows. Set $H(\emptyset)$ (the empty word) = \emptyset (the empty tree). If $w \neq \emptyset$, let m be the largest element of w , so w can be written uniquely as umv , where u and v are partial permutations (possibly empty). Set m to be the root of $H(w)$, with $H(u)$ its left subtree and $H(v)$ its right subtree.

The heap of a permutation will turn out to be a *decreasing binary tree*, i.e., the labels along any path from the root form a decreasing sequence. For more information, see the equivalent definition of *increasing binary tree* and the results thereafter in [19, §1.5].

Example 9. The heap associated with $w = 314975826$ is shown below.



We state the following very elementary facts without proof.

Proposition 10. Let $w \in \mathfrak{S}_n$ given in one-line notation have corresponding heap $H(w)$.

1. In $H(w)$, the left successor of j is the greatest element k to the left of j in w , such that all elements of w between k and j inclusive are $\leq j$.
2. The map $w \mapsto H(w)$ is a bijection between \mathfrak{S}_n and the set of decreasing binary trees (as defined above) with n vertices.
3. Let $\sigma \in \mathfrak{S}_S$, where $S = \{x_1 < x_2 < \dots < x_\ell\}$ is any finite totally ordered set. Let $\xi : S \rightarrow [\ell]$ be the canonical bijection $x_i \mapsto i$, which naturally extends to a bijection $\xi : \mathfrak{S}_S \rightarrow \mathfrak{S}_\ell$. We can use this map to extend the notions of dihedral symmetries, cycle structure, and the Rényi-Foata map \mathcal{F} to \mathfrak{S}_S , in particular to partial permutations of n .

We need the last statement above to be able to define and prove things recursively.

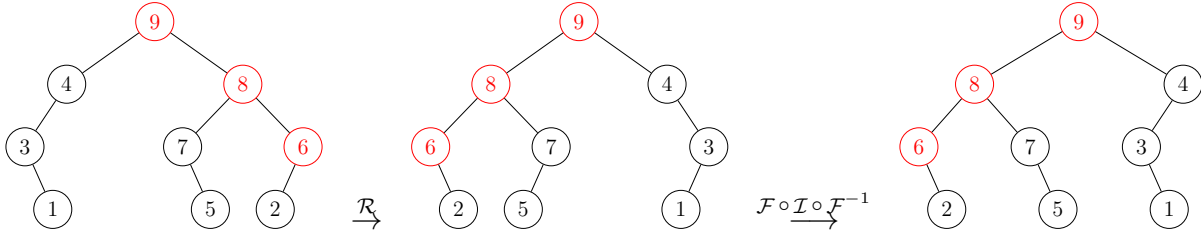
Example 11. Consider the partial permutation $\sigma = 753296$ of 9. We can consider this in two-line notation as $\sigma = \begin{pmatrix} 2 & 3 & 5 & 6 & 7 & 9 \\ 7 & 5 & 3 & 2 & 9 & 6 \end{pmatrix}$, and in CCD as $\sigma = (53)(9627)$. Here

$$\sigma^{-1} = \begin{pmatrix} 2 & 3 & 5 & 6 & 7 & 9 \\ 6 & 5 & 3 & 9 & 2 & 7 \end{pmatrix} = 654927 = (53)(9726).$$

Lemma 12. Let $w \in \mathfrak{S}_n$ have the form AnB (in one-line notation), where A and B are (possibly empty) partial permutations of n . Then the action of φ satisfies $\varphi(AnB) = \varphi(B)nA$. Thus, $H(\varphi(AnB))$ is the heap interchanging the left and right subtrees at the root vertex n , leaving the former unchanged and applying φ recursively to the latter. In particular, the action of φ preserves the underlying unlabeled graph of the corresponding heaps.

Proof. We analyze step-by-step how $\varphi = \mathcal{F} \circ \mathcal{I} \circ \mathcal{F}^{-1} \circ \mathcal{R}$ acts on the word $w = AnB$, using $w = 314975826$ (from Example 9) as a running example. First we see straight from the definitions that \mathcal{R} acts on the heap by switching left and right at each vertex, yielding the middle diagram in Figure 2.

Figure 2: The action of reversal-inclusion on the heap of the permutation $w = 314975826$.



Here we mark in red the sequence of records of $\mathcal{R}(w) = 628579413$, which were the original right-to-left maxima in w . These will be exactly those elements starting a cycle (following a left-parenthesis) in $\mathcal{F}^{-1}(\mathcal{R}(w)) = (62)(857)(9413)$. Applying \mathcal{I} to this (maintaining CCD) reverses the elements to the right of the first/largest element within each cycle, e.g., $\mathcal{I}(\mathcal{F}^{-1}(\mathcal{R}(w))) = (62)(875)(9314)$. Finally, applying \mathcal{F} drops parentheses, leaving the same set of records as before (for $\mathcal{R}(w)$), e.g., $\varphi(w) = 628759314$.

In the subtree of the original left subword $A = 314$, left and right were switched by \mathcal{R} , then back again by $\mathcal{F} \circ \mathcal{I} \circ \mathcal{F}^{-1}$; hence, the resulting right-subtree of the maximal element in the heap of $\varphi(w)$ is simply A . Whereas the subtree of the original right subword $B = 75826$ has become the left-subtree of the heap of $\varphi(n)$, but with φ applied to it. The action of \mathcal{R} switches left and right children at each vertex, while $\mathcal{F} \circ \mathcal{I} \circ \mathcal{F}^{-1}$ switches back the children at every node except the records. In particular, if $B = CmD$ with maximum m , then m becomes a record of $\mathcal{R}w$ so $\mathcal{F} \circ \mathcal{I} \circ \mathcal{F}^{-1}$ undoes the swapping at every vertex derived from C , while the vertices derived from D are restored accordingly as they would have been were n and A empty. The net effect is that $\varphi(AnB) = \varphi(B)nA$.

The resulting heap will have the same underlying *unlabeled graph structure* as the original heap, but does not preserve the *binary tree* structure, since some left edges become right edges, while others stay the same. ■

Definition 13. Let T be unlabeled binary tree with n vertices. For every vertex v of T , let τ_v be the map that interchanges (toggles) the left and right subtrees of T . Let $\Gamma(T) = \langle \tau_v : v \in T \rangle$ be the subgroup generated by these involutions, which we can think of as a subgroup of \mathfrak{S}_n of size dividing 2^n .

Note that φ acts as an element of $\Gamma(T)$, where $T = T(H(w))$ is the underlying unlabeled tree of the heap of a permutation.

The recursive structure described in the above lemma allows us to prove interesting facts about the orbit structure and that certain natural statistics are homomesic. The reader is invited to check each statement against the two orbits of $\bar{\varphi}$ displayed (with their heaps) in Figure 3. To view this as an action of φ itself, just drop all parentheses from the listed permutations.

Theorem 14. *The orbits of the action of $\bar{\varphi}$ (or φ) on \mathfrak{S}_n , satisfy the following properties.*

1. *The size of each φ -orbit (equivalently $\bar{\varphi}$ -orbit) is a power of 2. Specifically if w lies in the orbit, define the **height** of the heap $H(w)$ to be the number of edges h in a maximal path from the root (to a leaf); then the size of the orbit is 2^h . Consequently, as noted by Mike Joseph, the GCD of the orbit sizes is the greatest power of 2 that is less than or equal to n ; for if $2^k < n$, then any binary tree containing $1, 2, \dots, n$ has at least one vertex that is at least k steps away from the root.*
2. *Let $\text{Fix } w$ denote the number of fixed points, i.e., 1-cycles, of w . Then the statistic Fix is 1-mesic with respect to the action of $\bar{\varphi}$. Equivalently, $\text{Rasc} = \# \text{record-ascents}$ (see below) is 1-mesic with respect to the action of φ .*
3. *For fixed values $i \neq j$ in $[n]$, let $\mathbb{1}_{i < j}(u)$ denote the indicator statistic of whether i occurs to the left of j in the one-line notation of u . Then $\mathbb{1}_{i < j}$ is $\frac{1}{2}$ -mesic with respect to the action of φ .*
4. *Similarly for fixed $i \in [n]$, let $\mathbb{1}_{(i,n)}$ denote the indicator statistic of whether i and n lie in the same cycle of w . Then $\mathbb{1}_{(i,n)}$ is $\frac{1}{2}$ -mesic with respect to the action of $\bar{\varphi}$.*

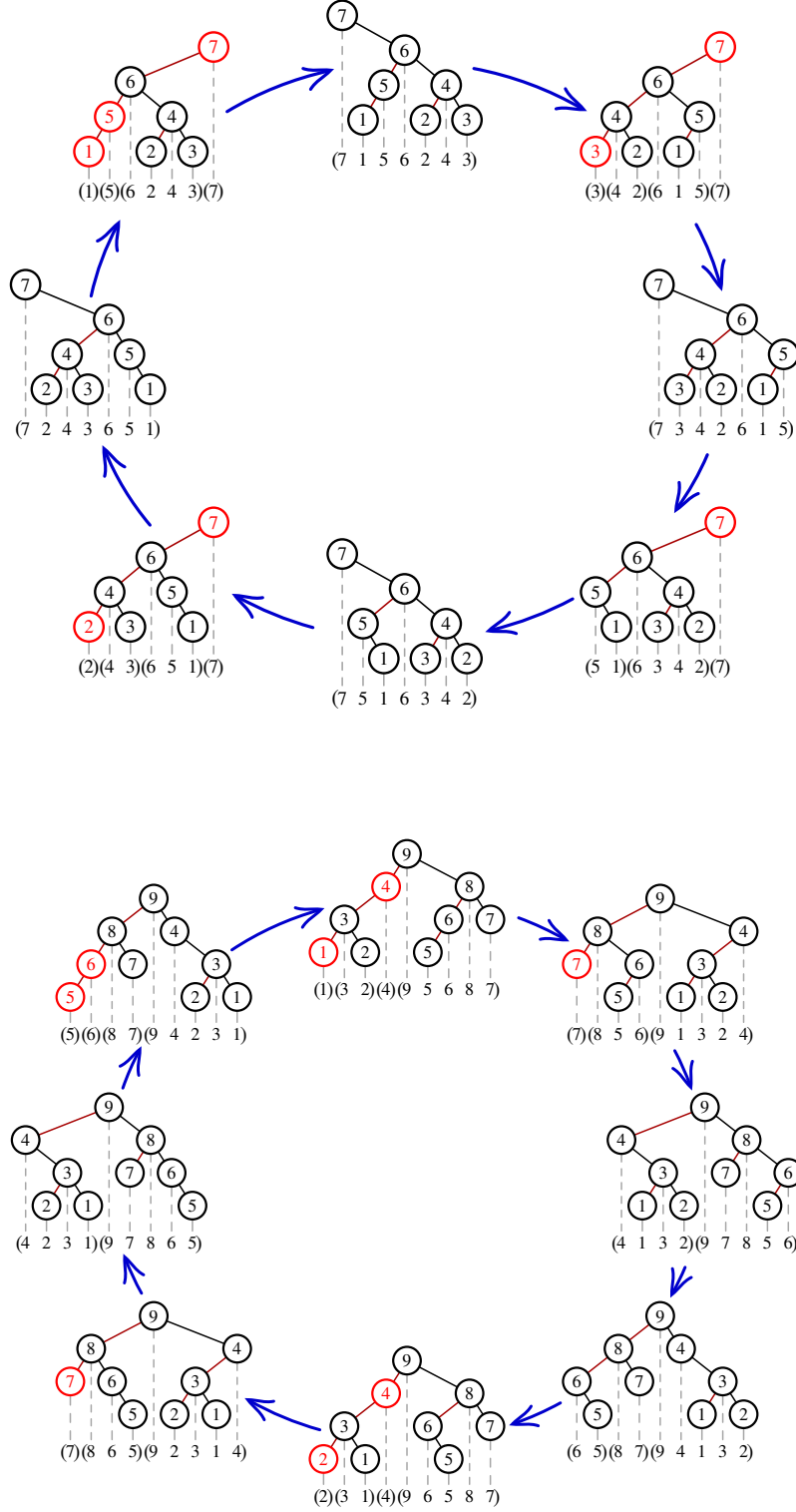
Proof. The proof of each statement proceeds by induction, using the lemma above, and assuming the statement is true for the action of φ on \mathfrak{S}_k for every $k < n$.

1. If $n = 1$, then there is only one orbit of size 1 (the base case). Otherwise, $w = AnB$ where at least one of A or B is nonempty. By Lemma 12, the action of φ on w looks as follows:

$$AnB \mapsto \varphi(B)nA \mapsto \varphi(A)n\varphi(B) \mapsto \varphi^2(B)n\varphi(A) \mapsto \varphi^2(A)n\varphi^2(B) \mapsto \dots \quad (6)$$

In order for the action to return to AnB , we must apply the action an even number of times, so the correct set of values lies to the left of n . The first time these values will be the same

Figure 3: Two orbits (one for \mathfrak{S}_7 , one for \mathfrak{S}_9) of the Foatic reversal-inclusion map $\bar{\varphi}$ with associated heaps, with **fixed points** marked in **red**. Each orbit has an average of one fixed point per permutation.



partial permutation as A is the size of the orbit of A in $\mathfrak{S}_{\#A}$, which by inductive hypothesis is a power of 2, say 2^a . (If A is empty, take $a = 0$.) Similarly for the values in B , which will return to their initial order after say 2^b steps. Thus, the size of the orbit of $w = AnB$ is $2 \cdot \text{LCM}(2^a, 2^b) = 2^{\max\{a,b\}+1}$. The heap of w has root n and subtrees $H(A)$ and $H(B)$. So assuming inductively that a represents the height of the heap of A and b that of B , the height of the heap of w is $\max\{a, b\} + 1$.

Note that in the case where exactly one of A or B is empty, we get that the orbit of AnB is exactly twice as long as that of the nonempty subword, e.g.,

$$An \xrightarrow{\varphi} nA \xrightarrow{\varphi} \varphi(A)n \xrightarrow{\varphi} n\varphi(A) \xrightarrow{\varphi} \varphi^2(A)n \xrightarrow{\varphi} n\varphi^2(A) \xrightarrow{\varphi} \dots$$

2. First note that the statement holds trivially for $n = 1$ and $n = 2$, where there is only a single orbit of φ . Also note that the statistic $\text{Fix } w$ translates to $\text{Rasc } \mathcal{F}(w)$ where for $u \in \mathfrak{S}_n$ given in one-line notation

$\text{Rasc } u := \#\{\text{records of } u \text{ immediately followed by another record or in the final position}\}.$

In other words, $\text{Rasc } u$ counts the number of records that are also *ascents*. For example, for $w = 847296513 = (42)(6)(81)(9375)$ as in Equation (1), $\text{Fix } w = 1$, and the 1-cycle (6) translates into the only record of $\mathcal{F}(w) = 426819375$ which is immediately followed by a larger entry. In particular, a nonempty substring to the right of n contributes nothing to $\text{Rasc } u$ (equivalently in $\mathcal{F}^{-1}(u)$ there are no 1-cycles to the right of n .)

We want to show that Rasc is 1-mesic on orbits of φ . Arguing as above, we claim that for $w = AnB$

$$\begin{aligned} \text{Average of Rasc across a } \varphi\text{-orbit} &= \frac{1}{2} \cdot \text{Average of Rasc across a } \varphi\text{-orbit of } A \\ &+ \frac{1}{2} \cdot \text{Average of Rasc across a } \varphi\text{-orbit of } B \quad (7) \\ &+ \frac{1}{2}, \text{ in the case that } A \text{ or } B \text{ is empty.} \end{aligned}$$

For the φ -orbit of w simply alternates the orbits of the substrings A and B to the left of n , with substrings to the right of n making no contribution. So each orbit contributes half of its average to the total. If one of the substrings is empty, then half the time n will contribute 1 to Rasc , otherwise n never contributes. By induction hypothesis, the average of Rasc across any orbit (hence superorbit) for either substring is one, and the result follows from (7).

3. The statement is clear for the single φ -orbit when $n = 2$. WLOG assume $i < j$. If i, j lie in different substrings, or if $j = n$, then clearly i alternates between being before or after n by Lemma 12. The remaining case is that i and j live in the same substring, say A , so their relative order is determined by their relative order in the substrings with the same elements as A in Equation (6), i.e., $A, A, \varphi(A), \varphi(A), \varphi^2(A), \varphi^2(A), \dots$. By induction, $\mathbb{1}_{i < j}$ is $\frac{1}{2}$ -mesic for the action of φ on A , so the same is true for the “orbit” where each element is repeated twice; equivalently, $\mathbb{1}_{i < j}$ is $\frac{1}{2}$ -mesic for the φ -orbit of $w = AnB$.

4. Clearly i alternates between being before or after n in the one line notation of $\mathcal{F}u = w = AnB$ by Lemma 12. This translates into an alternation of i and n being in the same cycle

Table 1: Data on orbit sizes for reversal-inversion

n	1	2	3	4	5	6	7	8	9	10	11
# of orbits:	1	1	2	5	19	84	448	2884	21196	174160	1598576
LCM of orbit sizes:	1	2	4	8	16	32	64	128	256	512	1024
GCD of orbit sizes:	1	2	2	4	4	4	4	8	8	8	8
Longest orbit size:	1	2	4	8	16	32	64	128	256	512	1024
Shortest orbit size:	1	2	2	4	4	4	4	8	8	8	8
Size of id's orbit:	1	2	4	8	16	32	64	128	256	512	1024

in u , since every element to the right of n in w ends up in the cycle with largest element n when \mathcal{F}^{-1} is applied. ■

Data on orbit sizes for φ are given in Table 1.

3 Complement-inversion

The next nicest Foatic action appears to be the one given by:

$$\bar{\gamma} : \mathfrak{S}_n \xrightarrow{\mathcal{F}} \mathfrak{S}_n \xrightarrow{\mathcal{C}} \mathfrak{S}_n \xrightarrow{\mathcal{F}^{-1}} \mathfrak{S}_n \xrightarrow{\mathcal{I}} \mathfrak{S}_n. \quad (8)$$

Example 15. Let $w = (2)(3)(514) \in \mathfrak{S}_5$ in CCD. Then the successive action of $\bar{\gamma}$ on w is detailed below:

$$\begin{aligned}
w = (2)(3)(514) &\mapsto 23514 \mapsto 43152 \mapsto (431)(52) \mapsto (413)(52) = \bar{\gamma}(w) \\
(413)(52) &\mapsto 41352 \mapsto 25314 \mapsto (2)(5314) \mapsto (2)(5413) = \bar{\gamma}^2(w) \\
(2)(5413) &\mapsto 25413 \mapsto 41253 \mapsto (412)(53) \mapsto (421)(53) = \bar{\gamma}^3(w) \\
(421)(53) &\mapsto 42153 \mapsto 24513 \mapsto (2)(4)(513) \mapsto (2)(4)(531) = \bar{\gamma}^4(w) \\
(2)(4)(531) &\mapsto 24531 \mapsto 42135 \mapsto (4213)(5) \mapsto (4312)(5) = \bar{\gamma}^5(w) \\
(4312)(5) &\mapsto 43125 \mapsto 23541 \mapsto (2)(3)(541) \mapsto (2)(3)(514) = \bar{\gamma}^6(w)
\end{aligned}$$

This example also displays (down the second column) the conjugate orbit of γ , also of size 6.

$$23514 \xrightarrow{\gamma} 41352 \xrightarrow{\gamma} 25413 \xrightarrow{\gamma} 42153 \xrightarrow{\gamma} 24531 \xrightarrow{\gamma} 43125 \mapsto$$

There are 6 fixed points distributed between the 6 permutations in this orbit: 2 is fixed by three permutations, and 3, 4, and 5 are fixed once each.

We examined all orbits of the action of γ on \mathfrak{S}_n for $n \leq 11$ and the number of fixed points was 1–mesic in every orbit we encountered. We also observed some interesting patterns to the orbit sizes, but were unable to prove any in generality. Data on orbit sizes in tabulated in Table 2.

Table 2: Data on orbit sizes for complement-inversion

n	1	2	3	4	5	6	7	8	9	10	11
# of orbits:	1	1	2	5	15	60	288	1656	11028	84042	717700
LCM of orbit sizes:	1	2	4	24	48	480	2880	40320	241920	50803200	101606400
GCD of orbit sizes:	1	2	2	2	2	2	2	2	2	2	2
Longest orbit size:	1	2	4	8	16	32	80	144	360	1260	2880
Shortest orbit size:	1	2	2	2	2	2	2	2	2	2	2
Size of id's orbit:	1	2	4	8	16	32	64	128	256	512	1024

The prime factorizations of the LCM of orbit sizes suggest a simple formula and hint at an underlying structure to the action, but we have been unable to make the pattern precise or identify such structure.

$$\begin{array}{llll}
1 = 1 & 24 = 2^3 \cdot 3 & 2880 = 2^6 \cdot 3^2 \cdot 5 & 50803200 = 2^9 \cdot 3^4 \cdot 5^2 \cdot 7 \\
2 = 2 & 48 = 2^4 \cdot 3 & 40320 = 2^7 \cdot 3^2 \cdot 5 \cdot 7 & 101606400 = 2^{10} \cdot 3^4 \cdot 5^2 \cdot 7 \\
4 = 2^2 & 480 = 2^5 \cdot 3 \cdot 5 & 241920 = 2^8 \cdot 3^3 \cdot 5 \cdot 7 &
\end{array}$$

The powers of 2 in the LCMs are achieved by the orbit containing the identity permutation in every case we have examined, but we do not have a simple way to show this is never exceeded, nor to explain the other prime factors.

Notice that when $n \geq 2$, the numbers 1 and n are in the same cycle of w if and only if they are in different cycles of $\gamma(w)$. It follows that every orbit has even length, and the indicator statistic $\mathbb{1}_{(i,n)}$ is $\frac{1}{2}$ -mesic. The GCD of the orbits is completely accounted for by noting that $\mathcal{R}(123 \cdots n)$ is in the unique 2-cycle created by the action of γ for every $n \geq 2$.

Conjecture 16. *The action of $\bar{\gamma}$ on \mathfrak{S}_n has the following properties.*

1. *The statistic Fix , which counts the number of fixed points (1-cycles), is 1-mesic.*

4 Complement-rotation

Our search of orbits for small n also failed to produce a counter-example to the conjecture that Fix is 1-mesic for the Foatic action given by:

$$\bar{\rho} : \mathfrak{S}_n \xrightarrow{\mathcal{F}} \mathfrak{S}_n \xrightarrow{\mathcal{C}} \mathfrak{S}_n \xrightarrow{\mathcal{F}^{-1}} \mathfrak{S}_n \xrightarrow{\mathcal{Q}^2} \mathfrak{S}_n. \quad (9)$$

Our observations about orbit sizes for ρ are tabulated in Table 3. A consequence of our choice of computing environment means that this tabulation is incomplete, since the LCM of orbit sizes could not be carried out using PostScripts native integers, but the prime factorization in the case $n = 7$ is sufficient to exclude any simple structures of the form discussed in the preceding two section.

We were surprised to observe from our data that every orbit of $\bar{\rho}$ had a representative permutation in which 1 appeared as a fixed point, but given the number of orbits we examined, we conjecture that this is a general property of orbits of $\bar{\rho}$.

Table 3: Data on orbit sizes for complement-rotation

n	1	2	3	4	5	6	7	8	9	10	11
# of orbits:	1	1	1	4	8	30	70	300	716	3360	7012
LCM of orbit sizes:	1	2	6	24	480	347760	$\sim 3 \times 10^{14}$	n/a	n/a	n/a	n/a
GCD of orbit sizes:	1	2	6	2	2	2	2	2	2	2	2
Longest orbit size:	1	2	6	8	32	108	576	2694	16864	116168	1676162
Shortest orbit size:	1	2	6	4	6	6	10	10	12	12	14
Size of id's orbit:	1	2	6	8	10	12	14	16	18	20	22

The LCM for $n = 7$ has the exact value $295162920561600 = (2)^6(3)^4(5)^2(7)(13)(23)(67)(109)(149)$. Entries of n/a reflect the fact that our initial computations were carried out using the PostScript programming language, and intermediate calculations exceeded the maximum value of an integer in our interpreter. The values should be easily accessible to any serious reimplementer of the computation.

Table 4: Data on orbit sizes for complement-rotation

n	1	2	3	4	5	6	7	8	9	10	11
# of orbits:	1	1	1	4	8	26	50	222	378	2356	3634
LCM of orbit sizes:	1	2	6	24	4680	155195040	1768492025501160960	n/a	n/a	n/a	n/a
GCD of orbit sizes:	1	2	6	2	2	2	2	2	2	2	2
Longest orbit size:	1	2	6	8	36	102	726	1216	9656	20050	160128
Shortest orbit size:	1	2	6	4	6	4	8	8	12	12	12
Side if id's orbit:	1	2	6	6	36	28	70	96	4312	3784	19784

Conjecture 17. *The action of $\bar{\rho}$ on \mathfrak{S}_n has the following properties.*

1. *The statistic Fix, which counts the number of fixed points (1-cycles), is 1-mesic.*
2. *Each orbit contains at least one permutation with 1 as a fixed point (aka (1) as a 1-cycle).*
3. *There is a natural indicator statistic that is $\frac{1}{2}$ -mesic and accounts for the orbits having even size.*

5 Reversal-rotation

The only remaining Foatic action for which Fix is potentially 1-mesic is

$$\bar{\tau} : \mathfrak{S}_n \xrightarrow{\mathcal{F}} \mathfrak{S}_n \xrightarrow{\mathcal{R}} \mathfrak{S}_n \xrightarrow{\mathcal{F}^{-1}} \mathfrak{S}_n \xrightarrow{\mathcal{Q}^2} \mathfrak{S}_n. \quad (10)$$

Our data on the sizes of orbits is tabulated in Table 4.

Conjecture 18. *The statistic Fix, which counts the number of fixed points (1-cycles), is 1-mesic for the action of τ on \mathfrak{S}_n .*

6 Other Foatic maps

The remaining 21 Foatic actions as described in Section 1.2 all fail to have Fix as a 1-mesic statistic and fall outside of the scope of our initial investigation. The dynamics of these action have been further studied, however, by Elizabeth Sheridan Rossi in her doctoral dissertation [18], where she considered a wider range of statistics, as outlined in Section 1.4.

7 Data Availability

Part of this investigation was accomplished using programs written in the PostScript programming language. PostScript is not usually considered suitable for serious mathematical research, but it was sufficiently flexible for the early stages of this project. One such program is currently available from the first author’s webspace

<https://math.mit.edu/~malacroi/permHomomesyFoaticFP/FoaticActions.txt>

It is designed to be run using the *GhostScript* interpreter, and could be invoked as follows.

```
gs -dNODISPLAY -dusecycles=true -dmaxpl=8 FoaticActions.txt
```

```
gs -dNODISPLAY -dshoworbits=true -dmaxpl=6 FoaticActions.txt
```

```
gs -dNODISPLAY -donlygood=true -dmaxpl=10 FoaticActions.txt
```

In our initial investigation, we permitted Q and Q^3 to take the roles of \mathcal{A} and \mathcal{B} , so our data involves 49 distinct actions. Some output is also available for interested parties. A tabulation of all of the orbits acting on permutations of order at most 6 can be found at

<https://math.mit.edu/~malacroi/permHomomesyFoaticFP/AllOrbits1-6.txt>

While a corresponding tabulation of the 4 actions conjectured to have Fix as a homomesy can be found at

<https://math.mit.edu/~malacroi/permHomomesyFoaticFP/GoodOrbits1-8.txt>

References

- [1] D. Armstrong, C. Stump, and H. Thomas, *A uniform bijection between nonnesting and noncrossing partitions*, Transactions of the American Mathematical Society **365** (2013), no. 8, 4121–4151, Also available as [arXiv:1101.1277v2](https://arxiv.org/abs/1101.1277v2).
- [2] Jonathan Bloom, Oliver Pechenik, and Dan Saracino, *Proofs and generalizations of a homomesy conjecture of Propp and Roby*, Discrete Math. **339** (2016), no. 1, 194–206, <https://doi.org/10.1016/j.disc.2015.08.011>.
- [3] Miklós Bóna, *Combinatorics of permutations*, Discrete Mathematics and its Applications (Boca Raton), Chapman & Hall/CRC, Boca Raton, FL, 2004, <https://doi.org/10.1201/9780203494370>, With a foreword by Richard Stanley.
- [4] D. Einstein and J. Propp, *Combinatorial, piecewise-linear, and birational homomesy for products of two chains*, Preprint (2018), [arXiv:1310.5294v3](https://arxiv.org/abs/1310.5294v3).

- [5] David Einstein, Miriam Farber, Emily Gunawan, Michael Joseph, Matthew Macauley, James Propp, and Simon Rubinstein-Salzedo, *Noncrossing partitions, toggles, and homomesies*, Electron. J. Combin. **23** (2016), no. 3, Paper 3.52, 26, <https://doi.org/10.37236/5648>, Also available at [arXiv:1510.06362v2](https://arxiv.org/abs/1510.06362v2).
- [6] Dominique Foata and Marcel-P. Schützenberger, *Théorie géométrique des polynômes eulériens*, Lecture Notes in Mathematics, Vol. 138, Springer-Verlag, Berlin-New York, 1970.
- [7] D. Grinberg and T. Roby, *Iterative properties of birational rowmotion II: rectangles and triangles*, Electron. J. Combin. **22** (2015), no. 3, Paper 3.40, 49.
- [8] ———, *Iterative properties of birational rowmotion I: generalities and skeletal posets*, Electron. J. Combin. **23** (2016), no. 1, Paper 1.33, 40.
- [9] M. Joseph and T. Roby, *Toggling independent sets of a path graph*, Electron J. Combin. **25** (2018), no. 1, 1–18, Also available at [arXiv:1701.04956v2](https://arxiv.org/abs/1701.04956v2).
- [10] ———, *Birational and noncommutative lifts of antichain toggling and rowmotion*, Algebr. Comb. (to appear) (2020), [arXiv:1909.09658v3](https://arxiv.org/abs/1909.09658v3).
- [11] Michael Joseph, *Antichain toggling and rowmotion*, Electron. J. Combin. **26** (2019), no. 1, Paper No. 1.29, 43.
- [12] James Propp and Tom Roby, *Homomesy in products of two chains*, Electron. J. Combin. **22** (2015), no. 3, Paper 3.4, 29, Also available at [arXiv:1310.5201v5](https://arxiv.org/abs/1310.5201v5).
- [13] V. Reiner, D. Stanton, and D. White, *The cyclic sieving phenomenon*, Journal of Combinatorial Theory, Series A **108** (2004), no. 1, 17–50.
- [14] ———, *What is... cyclic sieving*, Notices Amer. Math. Soc **61** (2014), no. 2, 169–171.
- [15] Alfréd Rényi, *Théorie des éléments saillants d’une suite d’observations*, Ann. Fac. Sci. Univ. Clermont-Ferrand **8** (1962), 7–13.
- [16] Tom Roby, *Dynamical algebraic combinatorics and the homomesy phenomenon*, in Recent trends in combinatorics, IMA Vol. Math. Appl., vol. 159, Springer, [Cham], 2016, Also available at <http://www.math.uconn.edu/~troby/homomesyIMA2015Revised.pdf>, pp. 619–652, https://doi.org/10.1007/978-3-319-24298-9_25.
- [17] D. Rush and K. Wang, *On orbits of order ideals of minuscule posets II: Homomesy*, Preprint (2015), [arXiv:1509.08047](https://arxiv.org/abs/1509.08047).
- [18] Elizabeth Sheridan Rossi, *Homomesy for Foatic actions on the symmetric group*, Ph.D. thesis, University of Connecticut, 2020.
- [19] Richard P. Stanley, *Enumerative combinatorics. Volume 1*, second ed., Cambridge Studies in Advanced Mathematics, vol. 49, Cambridge University Press, Cambridge, 2012, Also available at <http://math.mit.edu/~rstan/ec/ec1/>.

- [20] J. Striker and N. Williams, *Promotion and rowmotion*, European J. Combin. **33** (2012), 1919–1942, Also available at [arXiv:1108.1172v3](#).
- [21] Jessica Striker, *Rowmotion and generalized toggle groups*, Discrete Math. Theor. Comput. Sci. **20** (2018), no. 1, Paper No. 17, 26, Also available at [arXiv:1601.03710v5](#).
- [22] H. Thomas and N. Williams, *Rowmotion in slow motion*, Proceedings of the London Mathematical Society **119** (2019), no. 5, 1149–1178.